International Journal of Computational Methods and Experimental Measurements
https://www.acadlore.com/journals/IJCMEM

Comprehensive Study on the Influence of Shot Peening Duration on the Mechanical Behavior of Aluminum Alloy AA6061-T6 Exposed to Alkaline Environment

Khadir Mouaid Khudhair, Mohammed Abdulraoof Abdulrazzaq, Ali Mohammed Flayyih*

Department of Materials Engineering, College of Engineering, Mustansiriyah University, 10045 Baghdad, Iraq

* Correspondence: Ali Mohammed Flayyih (ali.iq7840@uomustansiriyah.edu.iq)

Received: 11-12-2025 **Revised:** 12-17-2025 **Accepted:** 12-24-2025

Citation: K. M. Khudhair, M. A. Abdulrazzaq, A. M. Flayyih, "Comprehensive study on the influence of shot peening duration on the mechanical behavior of aluminum alloy AA6061-T6 exposed to alkaline environment," *Int. J. Comput. Methods Exp. Meas.*, vol. 13, no. 4, pp. 831–844, 2025. https://doi.org/10.56578/ijcmem130407.

Abstract: This work provides a comprehensive evaluation of the effect of shot peening (SP) time on the mechanical, electrochemical, and surface properties of AA6061-T6 aluminum alloy tested in an alkaline chloride medium (pH = 9). The specimens were subjectively peened for varying durations from 0 to 12 min. The subsequent effects on tensile strength, fatigue life, corrosion resistance, surface roughness, and microhardness were studied. The results showed that a SP time of 9 min increased the tensile strength and hardness through strain hardening, dislocation accumulation, and establishment of compressive residual stress. The formation of a strong passive layer and delayed crack initiation also help make the material more resistant to corrosion and fatigue. However, peening for more than 9 min resulted in rough and localized damage and slightly reduced the mechanical performance. The results show that a 9-minute SP duration is the ideal method to strengthen the surface and maintain a strong structure, which makes AA6061-T6 parts last longer under harsh conditions.

Keywords: Aluminum alloy; SP; Corrosion; Fatigue; Surface roughness

1 Introduction

Aluminum alloys are among the most popular materials in modern engineering because of their low density, high specific strength, and inherent corrosion resistance. Owing to its balance of mechanical performance and workability, AA6061-T6 is a good choice in this family and is used as a preferential material in automotive, marine, and aerospace components that are regularly subjected to chemically aggressive environments and variable loads. The protection provided by the oxide films of these alloys and the characteristics of their surface microstructures affect their stability, which in turn influences their longevity. In an alkaline environment, the localized form of corrosion, including pitting, intergranular attack, and stress-corrosion cracking, may develop where hydroxide ions have a faster rate of dismantling these protective layers, threatening the fatigue life and structural integrity of the alloy. Owing to these challenges, surface treatment technologies capable of enhancing the life of aluminum alloys and corrosion properties in harsh service environments are receiving increasing research attention [1–3].

Among the popular methods applied to modify the surface properties, thereby improving the corrosion and fatigue properties of metallic materials, shot peening (SP) is one of the most common surface modification techniques. The objective of SP is to create plastic deformation and compressive residual stresses by bombarding the metallic surface with spherical media at a high rate. Though there are several benefits associated with the refinement of the metallic surface by SP to improve the strength by making it harder, the compressive residual stresses generated by this process restrain the initiation and propagation of cracks [1, 2]. Moreover, the process alters the distribution of defects, surface morphology, and grain boundaries, which influences the electrochemical reactivity of the material in a corrosive environment. For these reasons, SP is becoming more flexible for use in aluminum alloys such as AA6061-T6, where the combination of extended fatigue and reduced weight design is essential for high-performance use, as well as in steel and titanium alloys [3, 4].

SP is one of the most critical yet least comprehended contributors to the overall effectiveness of this widely used treatment. The intensity and magnitude of the generated compressive stress field, roughness, and hardness of

the surface depend on the duration of exposure during peening. Excess exposure can result in overpeening, which may induce unwanted effects like embrittlement of the surface, microcracking, and destruction of integrity of the passive oxide layer. This might result from a narrow compressive zone range and be unable to provide sufficient strengthening [5, 6]. Therefore, the issue of the optimal peening time that allows a concurrent increase in the fatigue strength and corrosion resistance remains an important topic for engineers and researchers dealing with AA6061-T6.

It has been observed in other research that SP is highly efficient for the fatigue strength improvement of aluminum alloys due to the multiplication of dislocations in the surface layer and the refining of the grains [7, 8]. However, studies on the association between corrosion behavior in alkaline media and peening time have not been adequate. Aluminum oxide films are more easily dissolved in alkaline solutions and occur more frequently in industrial and marine environments. They also subjected the substrate to anodic solution. The compressive residual stress caused by SP can alter the electrochemical response. In case there is less surface imperfection, the decreased corrosion can be the speeding down of the anodic activity, and in case too much roughness or microcracks are formed, the corrosion can be increased. Thus, to optimize the treatment parameters of AA6061-T6 in practice, it is necessary to study how the interaction between SP duration, surface morphology, and corrosion mechanisms can affect the results [9, 10].

Although the duration is often assumed to be a fixed variable or a secondary variable, the literature indicates that SP parameters, including shot size, influence velocity, and coverage, have an influence on fatigue performance and electrochemical stability. Inappropriate peening may enhance the amount of available surface to conduct anodic reactions, and controlled SP has been established to favor the creation of stable passive films that restrict the density of the corrosion currents [11]. A limited number of studies have combined electrochemical measurements with mechanical fatigue measurements in a systematic way to obtain the entire behavior of peened alloys in the presence of an alkali, which is important given that electrochemical measurements with potentiodynamic polarization and electrochemical impedance spectroscopy (EIS) have already been determined to be useful for the quantitative measurement of such effects [12, 13]. Moreover, the energy input and exposure time can also significantly influence the pattern of deformation in the subsurface, which in turn determines the long-term resistance to corrosion, although methods such as laser shock peening (LSP) and microshot peening can be used with similar mechanisms of stressing the surface [14–16].

This study addresses the gap in the science of this study. Although SP has been reported to augment mechanical endurance, its effects on the fatigue life and kinetics of AA6061-T6 corrosion under alkaline conditions have not been fully studied. Complex relationships would require advanced knowledge of these relationships to determine a processing window that would ensure optimal performance. Thus, this study aimed to demonstrate how different periods of SP modify grain morphologies, residual stress fields, and surface and subsurface structures, and how it changes the fatigue performance and corrosion behavior. The aim of this study was to develop a mechanistic model that relates SP duration to degradation behavior under composite mechanical and chemical stress by using electrochemical parameters, including corrosion potential and current density, to correlate with fatigue test results and surface characterization [17].

The primary objective of this study was to determine the best SP time for AA6061-T6 to maximize its fatigue life and corrosion resistance in an alkaline environment. These include determining corrosion rates using EIS and polarization tests, determining the fatigue life with cyclic loading, surface profilometry, and microscopy to trace the history of the microstructure of peened surfaces. A set of studies provided the most effective time of peening to the desired service condition, which provides a quantitative model for understanding the trade-off between corrosion protection on one hand and mechanical strengthening.

The realization of such optimization has a direct impact on component design and maintenance from an industrial perspective. The prolongation of service life and reduction of maintenance expenses are vital in the case of aluminum alloys that are subjected to seawater or alkaline cleaning agents in auto frames, aircraft outfits, and marine fittings. A better understanding of the SP process helps achieve sustainable engineering by reducing the material waste and energy used to overprocess or prematurely fail a component. These findings may also guide the introduction of SP into composite surface technologies, including coating or anodizing, offering new opportunities for multipurpose systems of protection, which would combine a high level of corrosion resistance with mechanical enhancement.

Lastly, this paper addresses one of the key areas of intersection between materials science and engineering practices. The explanation of the complex relationships between the fatigue behavior, corrosion processes, and SP time not only contributes to simple knowledge, but also provides some practical recommendations for improving surface treatment strategies. The experimental outcomes are expected to inform future standards and design requirements of aluminum alloy components under cyclic and corrosive conditions to promote greater reliability and extended working life of such components. This work bridges a large gap in the current literature and develops the current knowledge of AA6061-T6 alloys in alkaline environments for academic or industrial use by systematically correlating the duration of surface treatment and its performance in fatigue corrosion.

2 Experimental Work

2.1 Material Selection and Characterization

This study used an aluminum alloy, AA6061-T6, with a high specific strength, excellent corrosion resistance, and favorable weldability, which is a precipitation-hardened Al-Mg-Si alloy with large-scale utilization in structural applications in the automotive, marine, and aerospace industries. The State Company for Inspection and Engineering Rehabilitation (SIER), Iraq, opted to ascertain the chemical compositions of the samples using optical emission spectroscopy (OES). Table 1 shows that the measured values are in good agreement with the ASTM B209 requirements [18].

Table 1. Chemical composition of AA6061-T6 aluminum alloy

Element	ASTM B209 (wt%)	Experimental (wt%)
Si	0.4–0.8	0.67
Fe	≤ 0.7	0.546
Cu	0.15–0.40	0.214
Mn	≤ 0.15	0.126
Mg	0.8–1.2	1.134
Cr	0.04–0.35	0.268
Zn	≤ 0.25	0.285
Ti	≤ 0.15	0.13
Al	Balance	93.2

To guarantee minimal thermal distortion, the alloy was received in plate form and laser-cut to standard dimensions. To remove machining irregularities and obtain a smooth surface finish, the surface was mechanically ground with abrasive papers of up to 2000 grit diameter of SiC and polished with diamond paste using a mirror.

2.2 Grouping and Specimen Geometry

Fifty specimens, each measuring 100 × 10 × 1.68 mm, were prepared. The specimens were divided into five groups based on the SP time: 0, 3, 6, 9, and 12 min.

Ten specimens per group were used to guarantee statistical reliability of the results. Before testing, all the specimens underwent the same stress-relieving, cleaning, and preparation processes.

2.3 Reduction of Stress Heating

The resulting mechanical and electrochemical reactions may be negatively affected by the residual stresses from machining. Consequently, all specimens underwent an hour-long stress-relieving annealing process at 343°C, after which they were allowed to cool naturally to room temperature. The process was carried out in a digitally controlled electric furnace at the Materials Engineering Department of Mustansiriyah University. In mechanical testing, this step reduces experimental scatter and guarantees a uniform microstructure.

2.4 Treatment with SP

At the Institute of Technology, Baghdad, a pneumatic tumble-blast control system was used to perform the SP procedure. To cause near-surface plastic deformation, hardened steel shots with a diameter of 1 mm and a hardness of 55 HRC were fired onto the specimen surface. Table 2 summarizes the process parameters.

Table 2. Operating parameters of the SP process

Process	Parameter
Shot material	Hardened steel
Shot diameter	1 mm
Shot hardness	55 HRC
Impact velocity	20 m/s
Air pressure	5 Bar
Nozzle inclination	10° from vertical
Standoff distance	100 mm
Surface coverage	100%
Peening durations	3, 6, 9, and 12 minutes

The treatment created a compressive residual stress field close to the surface, which should make it last longer and resist corrosion more effectively. Too much peening time can cause over-peening and make the surface brittle; therefore, different durations were chosen to determine the best exposure time.

2.5 Getting the Corrosive Medium Ready

A synthetic alkaline chloride solution was prepared to mimic alkaline marine conditions. This was done by dissolving 3.5 wt% NaCl in 1 L of distilled water and then slowly adding 10% $NaHCO_3$ solution until the pH reached 9.0 ± 0.1, which was checked with a calibrated pH meter. This environment encourages localized corrosion, which is similar to that of aluminum alloys when they are in industrial or coastal environments. For all the electrochemical tests, the temperature was maintained at 25 ± 2°C.

2.6 Electrochemical Characterization

A CS 310 CorrTest Workstation (Wuhan, China) was used to perform electrochemical measurements in a standard three-electrode cell setup, which included the following:

The working electrode was an AA6061-T6 specimen with an exposed area of 1 cm^2.

A Saturated Calomel Electrode (SCE) as the reference electrode and a platinum mesh was used as the counter electrode.

The electrolyte was used to soak all specimens for 30 min to obtain a stable open-circuit potential (OCP). Subsequently, potentiodynamic polarization (Tafel) scans were performed over a potential range of ±250 mV vs. OCP at a rate of 1 mV/s. Using Tafel plots, we determined the corrosion current density, corrosion potential, and corrosion rate according to ASTM G102 [19] using the following equation:

$$CR = 3.27 \times 10 - 3 \times \rho \; icorr \times EW/\rho \tag{1}$$

where, EW is the equivalent weight (g/equiv) and ρ is the density ($\mathrm{g/cm}^3$). These parameters were employed to assess the impact of the SP duration on the corrosion resistance.

2.7 Integrated Experimental Methodology and Research Strategy

The research approach adopted has been designed to conclude an experiment through an integrated research strategy that assesses systematically the impact of SP duration on surface modification and its subsequent impact on mechanical properties as well as corrosion performance. Surface characterization techniques (surface roughness and micro-hardness) have been adopted to confirm and assess systematically the impact of SP on surface modification. Mechanical assessment has been done by conducting tensile and fatigue testing to assess systematically the impact of surface modification on its mechanical performance. At the same time, electrochemical testing has been conducted systematically to assess its impact on corrosion performance. This research approach has been adopted to conclude an experiment through an integrated research strategy that assesses systematically performance trade-offs and identifies an optimal SP duration.

2.8 Mechanical Testing

2.8.1 Testing for tensile strength

Tensile properties were estimated using a WDW200-E universal testing machine (capacity: 200 kN) at a crosshead speed of 1 mm/min, as stipulated in ASTM B557M [20]. To demonstrate that the heat-treated alloy was mechanically sound and to establish a baseline of information upon which the alloy would behave under stress, the results were used.

2.8.2 Fatigue Testing

Fatigue testing of specimens was conducted using the Hi-Tech HSM20 rotatory bending fatigue testing machine under constant amplitude loading and room temperature conditions. Each specimen was set up in cantilever fashion under cyclic loading ranging between 70 and 210 MPa. Cycles to failure (Nf) values of specimens subjected to different SP times were determined and S–N curve diagrams used to interpret the resulting fatigue resistance.

For the purpose of ensuring the repeatability and validity of the fatigue data, a set of several samples was tested for every stress level, as well as for every SP process. A total of 50 samples was considered for analysis in the course of the testing process, and the data for the fatigue lives represents the mean value of a series of tests. It must, of course, be considered that the nature of fatigue failure introduces a degree of randomness into the data collection process, such that a degree of scatter in the data will be present.

2.9 Characterization of the Surface

2.9.1 Roughness of the surface

A Pocket Surf Mahr profilometer was used to measure surface roughness. Measurements at three random points were taken on each specimen over a 4 mm sampling length, and the arithmetic mean roughness (Ra) was recorded. The aim of this test was to measure the changes in the landscape caused by different SP durations.

2.9.2 Testing for microhardness

Microhardness was determined using a Vickers microhardness (HV) tester (Innovatest, Netherlands) with a load of 200 g and dwell time of 10 s, according to ASTM E384 [21]. Each specimen was indented at five points at a young, evenly spread out point, and the mean HV was calculated to ascertain the extent to which the SP enhanced the surface.

2.10 Experimental Matrix and Data Integrity

Table 3 summarizes the experimental plans employed in the current study to ensure that the results were reproducible.

Table 3. Summary of experimental tests and corresponding parameters

Category	Test Type	Standard	Equipment	Key Parameters	Output
Mechanical	Tensile	ASTM B557M	WDW200-E	$1\ \mathrm{mm/min}$	UTS (MPa)
Mechanical	Fatigue	In-house	HSM20	70–210 MPa	S-N Curve
Corrosion	Tafel Polarization	ASTM G102	CS 310 CorrTest	$3.5\ \mathrm{wt\%\ NaCl}$, pH9	Ecorr, icorr, CR
Surface	Roughness	ISO 4287 [22]	Pocket Surf Mahr	$\mathrm{Ra}(\mu\mathrm{m})$	Surface texture
Surface	Microhardness	ASTM E384	Innovatest	200 g, 10 s	HV value
Surface	SP Treatment	-	Tumblast system	3–12 min, 20 $\mathrm{m/s}$	Residual stress depth

All the instruments were calibrated before testing, and the environment's temperature, humidity, and pH were monitored continuously. The tests were repeated several times to ensure that the findings were consistent and reproducible.

The experimental design was intended to be a hierarchical, integrated test strategy, rather than a series of discrete tests. The test parameter for investigation was identified to be the time period for the SP process, and the test was conducted by keeping all other processing test conditions the same, thus ensuring the individual effect of SP time. Surface characterization was the first test to determine the amount of the surface alteration, in addition to the test of its further transformation into structural properties by the use of mechanical tests. Finally, electrochemical tests were conducted to determine the sensitivity of the surface properties to alkaline corrosive conditions.

3 Results and Discussion

The following results are discussed in this study in a unified framework. The results from surface characterization are analyzed first to understand the extent of surface modification due to SP, which forms the basis of understanding the results of mechanical and electrochemical tests. The results from mechanical tests are correlated with the surface roughness and surface hardening effect, and the results from electrochemical tests are explained with respect to the modified surface. In this way, it is ensured that all results are collectively contributing towards understanding the prime research objective.

3.1 Effect of SP Times on Tensile Strength

Table 4 and Figure 1 show the tensile strengths of the AA6061-T6 aluminum alloy samples before and after the SP process. The findings indicated that the untreated specimen exhibited the lowest ultimate tensile strength (UTS) owing to the lack of surface enhancement and compressive residual stresses. After SP, the tensile strength increased slowly over time, reaching its highest point after 9 min of treatment, and then decreased slightly after 12 min.

The increase in the UTS up to 9 min is due to the induced compressive residual stress field and the work-hardening effect of high-velocity shot impacts. These impacts cause considerable plastic deformation in the surface layer, which creates many dislocations and refines grains in certain areas. Both these factors make it harder for plastic to flow. Su et al. [15] say that micro-shot peening makes the surface crack initiation happen later by putting compressive stresses on the surface. This improved both the static and cyclic strengths. Similarly, Huang et al. [17] and Sheng-Li et al. [16] showed that a moderate amount of surface deformation makes aluminum alloys stronger and able to hold more weight.

After 12 min, a slight decrease in the tensile strength was observed. This reduction is directly proportional to the extreme roughing of the surface at this period. The roughness of the surface Ra shot up to 5.92 μm at 12 minutes, or 98 percent higher than the 9-minute sample, as shown in Section 3.4. These deep intersecting impact craters serve as

surface notches and stress concentrators, which undermine the integrity of the material and counteract the advantages of strain hardening. Sun et al. [14] similarly experienced this phenomenon. They determined that extensive laser or mechanical peening can cause local damage and increase the concentration of surface stress. Even after 12 min, the UTS was higher than that of the non-shot peened specimen. This shows that the overall mechanical improvement was greater than any small damage that occurred during longer peening times. Overall, the results showed that SP significantly increased the tensile strength of AA6061-T6. This is mostly because it hardens the surface, refines the grains, and leaves behind compressive stress. The best performance was achieved after 9 min of peening, which was the best balance between strengthening the surface and maintaining microstructure stability.

Table 4. Ultimate tensile strength of AA6061-T6 aluminum alloy before and after SP

Specimen	pH	Peening Time (min)	Peening Speed (m/s)	UTS (MPa)	Relative Change (%)
A	9	0	-	272	-
B	9	3	20	289	6.3
C	9	6	20	301	10.7
D	9	9	20	312	14.7
E	9	12	20	305	12.1

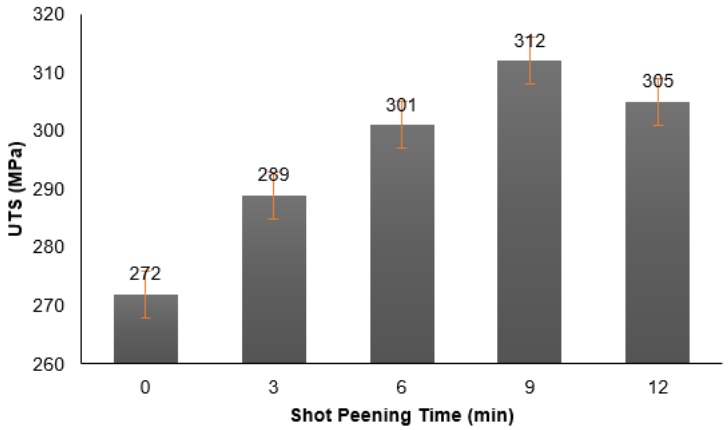

Figure 1. The outcomes of tensile strength for all samples

3.2 Effect of SP times on Corrosion Resistance

A 3.5 wt% NaCl alkaline solution (pH = 9) at room temperature was used in the experiment to assess the corrosion behavior of AA6061-T6 aluminum alloy of various SP durations. The electrochemical parameters obtained using the polarization curves are indicated in Table 5, and the resultant polarization curves are indicated in Figure 2. The highest density of corrosion current (icorr = 77.17 $\mu\mathrm{Acm}^{-2}$) and corrosion potential (-0.729 V) were found in the non-shot peened specimen (A) hence the highest corrosion rate of 0.84 mm y^{-1}. As the SP duration extended between 3 and 12 min, the density of the corrosion current diminished significantly to 21.27 $\mu\mathrm{Acm}^{-1}$ which caused the significant reduction of the corrosion rate to 0.24 mm y^{-1}. At the same time, Ecorr tended a slight movement in a more negative way, between -0.729 and -0.754 V, which demonstrates that SP mainly influences the corrosion kinetics, however, not the thermodynamic corrosion tendency. An analysis of polarization curves on Figure 2 shows that both the anodic and cathodic branches moved to lower current densities with increasing peening time which confirms the strong inhibition of the electrochemical reactions. This is explained by the fact that a dense, strain-hardened surface layer is formed as a result of SP which is usually linked with compressive residual stresses and grain refinement. This surface modification increases the stability of the protective oxide layer, decreases anodic dissolution and constraints the initiation and growth of pits. Li [5], Sun et al. [14], Su et al. [15], Sheng-Li et al. [16], and Huang et al. [17] are among the researchers who have reported similar improvements in corrosion resistance of surfaces that have been processed by the mechanically induced surface densification and stress effects. In general, the electrochemical findings indicate that the maximum level of the SP duration to a 12-minute level provides a significant improvement in the corrosion resistance of AA6061-T6 in alkaline environments (pH = 9), which is mostly achieved by a sharp decrease in the density of the corrosion current.

The lowest corrosion current density and most noble potential measured for specimen E confirmed that the optimized peening parameters (velocity = 20 ms^{-1}, shot diameter = 1 mm) successfully enhanced the surface compactness and passive-film integrity without causing over-peening effects.

Table 5. The Tafel electrochemical test before and after SP operation

Specimens	pH	Time of SP (min)	SP Speed (m/s)	Icorr (μA)	Ecorr (V)	Corr. Rate (mmpy)
A	9	0	-	77.171	-0.72948	0.84064
B	9	3	20	43.102	-0.73301	0.59621
C	9	6	20	31.186	-0.73989	0.44334
D	9	9	20	22.186	-0.74689	0.25121
E	9	12	20	21.27	-0.75442	0.24206

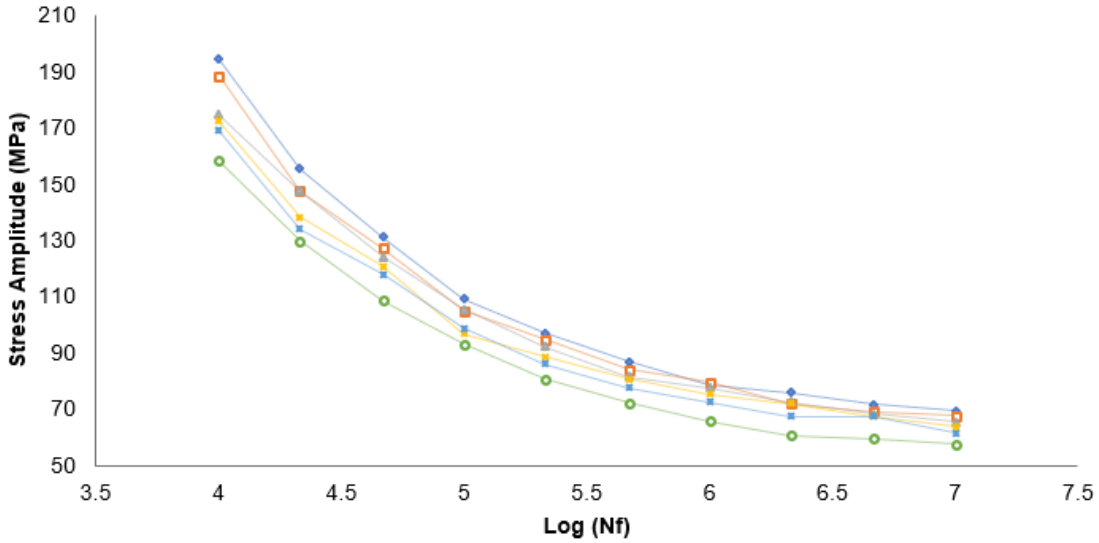

Figure 2. Tafel polarization curves of AA6061-T6 alloy after different SP durations

3.3 Effect of SP Times on Fatigue Life

The fatigue behavior of AA6061-T6 aluminum alloy specimens exposed to alkaline corrosion and subsequently treated by SP is presented in Table 6 and Figure 3 in the form of S–N curves. In all cases, corroded specimens exhibited lower fatigue lives than the uncorroded condition, confirming the detrimental effect of corrosion-induced surface damage on fatigue resistance. Surface pitting generated during alkaline exposure acts as a stress concentrator that accelerates crack initiation under cyclic loading.

SP significantly improved the fatigue performance of the corroded specimens compared with the non-shot peened condition. As shown in Table 6, the fatigue life increased progressively with increasing peening time from 3 to 9 min, reaching a maximum at 9 min, followed by a slight decrease at 12 min. Although some scatter in fatigue life was observed at identical stress levels, which is characteristic of fatigue testing, the overall trends were consistent across repeated tests, and the data dispersion remained within an acceptable range. This confirms that the observed improvements in fatigue life are systematic rather than random.

The enhancement in fatigue resistance can be rationalized by surface strengthening effects induced by SP, including work hardening and mechanisms commonly associated with compressive residual stress, as widely reported in the literature. These effects delay crack initiation and reduce the effective tensile stress acting at the surface [23]. The slight reduction in fatigue life observed after 12 min is attributed to over-peening, where excessive surface roughness and localized micro-damage introduce additional stress concentration sites that partially offset the beneficial surface strengthening effect [24].

As illustrated by the S–N curves in Figure 3, all SP corroded specimens exhibited longer fatigue lives than the non-shot peened corroded sample, with the 9 min treatment providing the most favorable balance between surface strengthening and roughness evolution. Despite the improvement achieved through SP, corrosion damage remained the dominant factor influencing fatigue performance, consistent with previous studies reported in the literature. Although, all the corroded samples had lower fatigue lives compared to the uncorroded sample, confirming that corrosion damage is still the primary factor affecting fatigue performance even after SP. These results agree with Sheng-Li et al. [16] and Su et al. [15], who stressed that SP significantly improves fatigue strength by inducing compressive stress, although its effectiveness is diminished in instances of severe corrosion damage. Similarly, Huang et al. [17] showed that the stability of residual stress in peened aluminum surfaces can decrease in harsh environments, making long-term fatigue improvement less likely.

Table 6. Fatigue tests of AA6061-T6 aluminum alloy specimens exposed to alkaline corrosion (pH = 9, 21 d) and subjected to SP

Log10 (Nf)	Nf (cycles)	Without Corrosion (SP=0)	NaCl (pH 9) SP 9 min	NaCl (pH 9) SP 6 min	NaCl (pH 9) SP 12 min	NaCl (pH 9) SP 3 min	NaCl (pH 9) SP 0 min
4	10000	194.5	188.6	174.8	172.5	169	158.4
4.33	21544	155.6	147.5	147.6	138.4	134	129.8
4.67	46415	131.2	127.3	124.3	120.7	118.1	108.7
5	100000	109.3	104.9	105.6	97	98.7	93.3
5.33	215443	97.1	95	92.3	88.6	86.1	80.9
5.67	464158	87.1	84.2	81.7	80.8	77.7	72.4
6	1000000	78.7	79.8	77.6	75.5	72.5	65.9
6.33	2154434	75.9	72	72.6	72.1	67.6	60.7
6.67	4641588	71.7	69.3	68.4	67.6	67.5	59.6
7	10000000	69.5	67.8	65.6	63.8	61.7	57.8

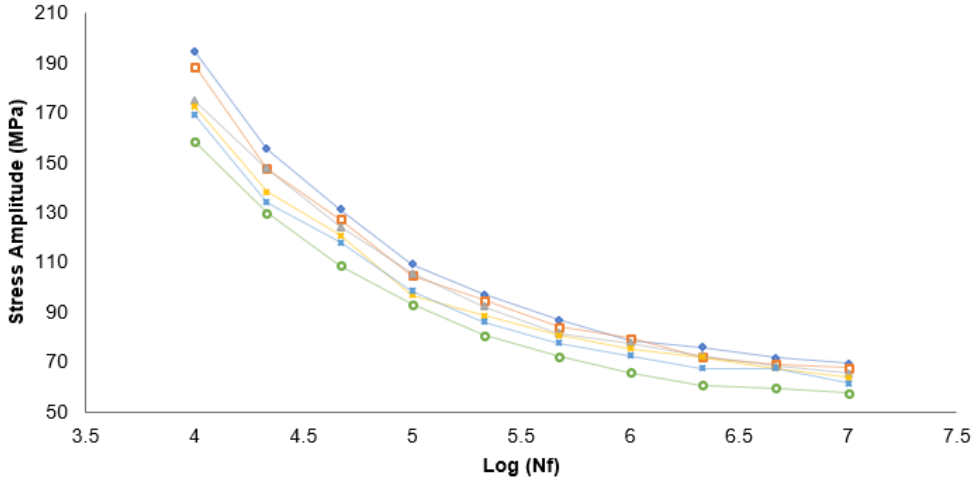

Figure 3. Fatigue life for all samples

The following Table 7 will describe a basic statistical treatment conducted on the fatigue data reported in Table 6 for giving a quantitative description of the dispersion of the data. For each condition, the stress values corresponding to fixed fatigue lives ($\log_{10}$ Nf = 4–7) were treated as a dataset. The mean value, standard deviation (σ), and coefficient of variation (CV) were determined. The computed coefficients of variation were included approximately between 36% and 39% for all testing conditions, that is, from the uncorroded specimen to the NaCl-exposed ones subjected to different SP durations. In detail, the non-shot peened specimen showed a coefficient of variation of about 38.8%, while SP specimens showed comparable dispersion levels (≈36–38%), which indicates that no excessive additional scatter was introduced by SP into the fatigue response. The obtained values are in good agreement with the intrinsically stochastic nature of the fatigue failure and fall within the range typically reported for Al alloys tested under rotating-bending fatigue conditions. Indeed, the similarity in dispersion among all conditions confirms that the observed improvements in fatigue life with increasing SP duration-particularly at 9 min-are systematic and physically meaningful rather than artifacts of experimental variability.

Table 7. Mean, standard deviation, and coefficient of variation of the stress of each condition at constant fatigue lives (Nf)

Condition	Mean Stress (MPa)	Std. Dev. (MPa)	CV (%)
Without corrosion (SP = 0)	107.1	41.5	38.8
NaCl (pH9), SP = 9 min	103.6	39.7	38.3
NaCl (pH9), SP = 6 min	101.1	37	36.6
NaCl (pH9), SP = 12 min	97.7	35.5	36.4
NaCl (pH9), SP = 3 min	95.3	35	36.8
NaCl (pH9), SP = 0 min	88.8	34	38.3

3.4 Effect of SP on Surface Roughness

ISO 4287 [22] was used to measure the Ra of corroded AA6061-T6 samples that had been in an alkaline environment (NaCl, pH 9) for different durations (0, 3, 6, 9, and 12 min). Table 7 shows the measured values, and Figure 4 shows them. The table and figure both show that Ra increased as the peening time increased. The average roughness increases from 1.667 μm for the non-shot peened surface (0 min) to 1.905 μm after 3 min, 2.528 μm at 6 min, 2.988 μm at 9 min, and 5.924 μm at 12 min.

There was a small increase in Ra between 0 and 3 min (+0.245 μm, 14%). Subsequently, it grew steadily for 9 min (+1.271 μm, ≈74%). At 12 min, there was a sharp increase (+98% compared to 9 min), which showed that the material was moving into over-peening, where overlapping impacts and excessive plastic deformation created deeper valleys and microcracks. The small difference between the repeated measurements (±0.02 μm) shows that the roughness data in Table 8 is very reliable and repeatable.

The surface roughness increased moderately from 3 to 9 min owing to the buildup of shallow dimples due to successive shots. During this period, positive compressive residual stresses (CRS) were prevailing, increasing the fatigue resistance and time for crack initiation by surface work hardening. These effects were similar to those of Table 6 and Table 3 [14, 15, 17] when there was a gain in the fatigue performance.

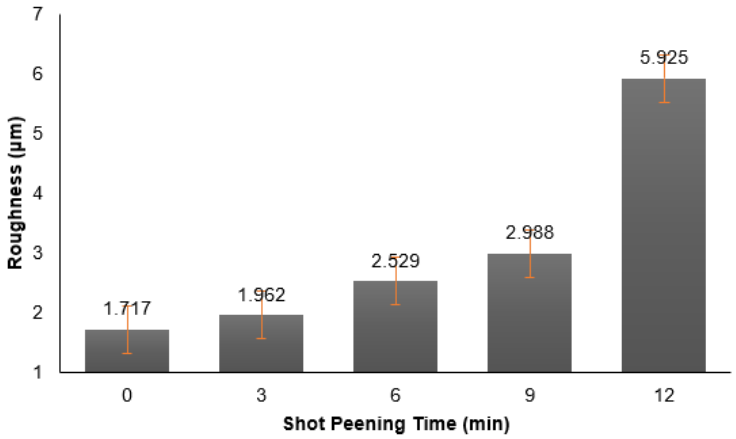

Figure 4. Surface roughness (μm) at different time of SP process in alkaline solution (pH 9)

Table 8. Results of roughness measurements for specimens with corrosion in solution (pH 9)

Specimen	Roughness (μm) (With Corrosion) at Different SP Times (min)				
	0 min	3 min	6 min	9 min	12 min
1	1.708	1.965	2.521	2.984	5.928
2	1.722	1.968	2.531	2.996	5.917
3	1.714	1.959	2.528	2.987	5.931
4	1.723	1.967	2.537	2.99	5.927
5	1.72	1.953	2.525	2.981	5.921
6	1.71	1.955	2.532	2.991	5.924
7	1.719	1.964	2.534	2.994	5.93
8	1.716	1.961	2.519	2.985	5.92
9	1.725	1.97	2.535	2.993	5.914
10	1.713	1.958	2.526	2.979	5.934
Average	1.717	1.962	2.529	2.988	5.925

The quantitative measure of over-peening can be considered to be the clear jump in Ra to 5.92 μm at 12 minutes. Such excessive roughness shows that the surface has become saturated and that further bombardment produces deep overlap craters instead of positive deformation. These geometrical irregularities efficiently decrease the cross-sectional area and introduce extreme stress concentration points, which is a physical explanation of the lower tensile and fatigue achievements being witnessed in the past sections [7, 14, 15]. The gradual increase in Ra also changed the occurrence of corrosion. Increased roughness increases the effective surface area and causes micro-valleys to trap chloride ions, which worsens pitting corrosion in alkaline NaCl solutions [16, 17]. However, for up to 9 min, the positive effect of CRS on the fatigue life was stronger than the negative effect of roughness. After this point,

the defects caused by roughness are removed, which lowers the fatigue performance. This is in line with previous findings for aluminum alloys that have been peened for a long time [14–17].

Figure 4 shows that the average Ra increases slowly until 9 min, and then jumps up quickly at 12 min. This pattern shows that 9 min is the best time for SP, because it strikes the best balance between the stress it causes and the surface shape it creates.

3.5 Effect of SP Time on Microhardness

Table 9 and Figure 5 show how the HV of the AA6061-T6 aluminum alloy samples changed when they were shot-peened for different durations in an alkaline medium (pH = 9). The findings indicate a gradual increase in the surface hardness, rising from 92 HV for the non-shot peened specimen to 117 HV after 9 min of SP, followed by a minor reduction to 114 HV at 12 min. This trend signifies that moderate SP exposure increases the near-surface mechanical properties by strain hardening, grain refinement, and the establishment of residual compressive stresses. The small decrease in the hardness at 12 minutes coincides with the limit extreme surface roughening Ra 5.92 μm. The excessive plastic deformation at this stage places in jeopardy the surface integrity, so that the surface texture is dominated by a series of peaks and valleys which are incapable of supporting the same localized indentation resistance as the smoother uniformly hardened 9-minute surface. The transient hardness rise to 9 min was due to the ongoing accumulation of dislocation density and the formation of fine-grained sub-grains in the surface layer that is deformed. These changes in the microstructure make it harder for dislocations to move and make the material less plastic, which increases the hardness values. Sun et al. [14], Su et al. [15], and Huang et al. [17] all reported similar results, showing that the best conditions for SP strengthen the surface the most without damaging the structure.

Table 9. Results of hardness measurements for specimens with corrosion in solution (pH 9)

Specimen	Microhardness (HV) with Corrosion				
	0 min	3 min	6 min	9 min	12 min
1	91.8	103.9	111	116.8	113.7
2	92.2	104.2	111.4	117.1	113.9
3	91.9	103.8	110.9	116.7	113.5
4	92.1	104	111.2	117	113.6
5	92	103.7	111.1	116.9	113.8
6	91.7	104.1	111.3	116.6	113.4
7	92.3	104.3	111.5	117.2	113.9
8	91.8	103.9	111	116.8	113.7
9	92.1	104.1	111.3	116.9	113.8
10	91.9	103.8	111.2	116.7	113.6
Average	91.98	104	111.19	116.87	113.68

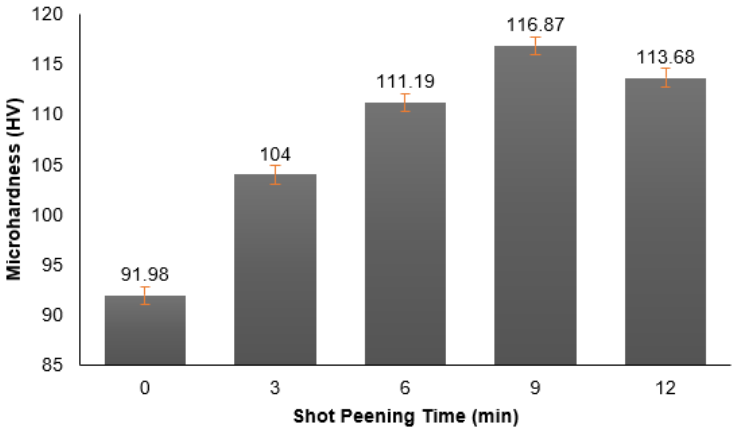

Figure 5. Surface hardness (HV) corrosion at different time of SP process in basic solution (pH 9)

However, if the peening time is longer than the optimal time (12 min), the impacts are too strong and cause surface craters, microcracks, and a partial release of compressive residual stresses. Therefore, although the surface roughness continued to increase, the microhardness decreased slightly. This decoupling occurs because the roughness growth shows that the surface has been deformed or damaged, whereas the hardness growth depends on subsurface strain

hardening and stress buildup. When the dislocation density reaches saturation, more impacts make the surface rougher rather than harder. Su et al. [15], and Huang et al. [17] also saw these over-peening effects in aluminum alloys.

The results demonstrate that 9-minute peening time is the best between hardening and keeping the surface rough enough. The measured value, according to ASTM E384 [21], shows that the controlled peening significantly increases the surface's integrity and resistance to mechanical stress without having the negative side effects of over-peening.

3.6 Integrated Mechanistic Framework Linking SP Time, Surface Modification, and Performance

Despite the fact that the mechanical, electrochemical and fatigue outcomes have been described individually, in the above sections, a concerted explanation is needed in a bid to understand the mechanism behind the reported tendencies. Figure 6 is a schematic representation of how the combined impacts of SP time on near-surface microstructural change, surface roughness development, residual strengthening, and the resultant mechanical and corrosion performance. This model allows to correlate the parameters of the processing directly with multifunctional properties.

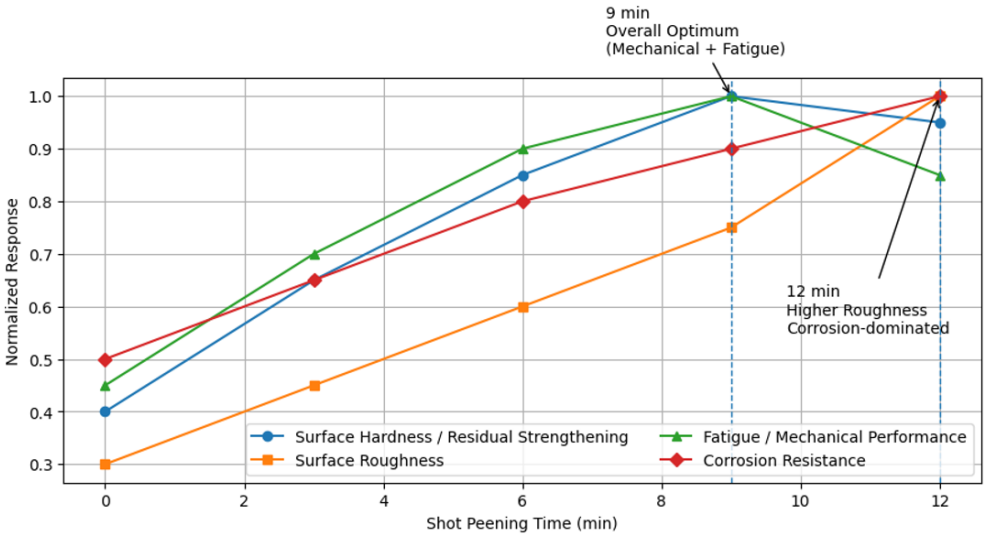

Figure 6. Schematic illustration of the integrated effect of SP time on surface roughness, residual strengthening, corrosion response, and fatigue performance

The effect of the increase in SP duration is an increase in the near-surface plastic deformation, and therefore an increase in the density of dislocations and increases in work hardening, which were determined by the increase in surface microhardness. This effect of strengthening is associated with tensile strength and fatigue resistance through a delay in crack initiation and inhibition of early plastic deformation. This advantageous process however attains a level of saturation with increasing peening times, beyond which, the extra effects no longer have a material strengthening effect but can cause surface damage.

Simultaneously with surface hardening, Ra also increases steadily as peening time increases, with a strong increase at 12 min, cancelling in part the positive effect of residual strengthening. This is the reason that the tensile strength and fatigue life would show a decrease after the optimal peening time (9 min) although the surface hardness would keep increasing.

Electrochemically, the correlation between corrosion resistance and peening time may be explained by the fact that a very deformed and compacted surface layer is formed, which facilitates the maintenance of the passive film; density of the corrosion current is lowered. The electrochemical response is less sensitive to surface roughness in the range of interest than fatigue performance and is more critically determined by the under-surface deformation and compressive residual effects. Corrosion resistance therefore keeps on increasing to 12 min, although mechanical performance has a minor decline owing to the roughness created by over-peening.

In order to explain more the quantitative relationships among surface modification, mechanical performance and corrosion behavior, a brief comparison of normalized experimental parameters was conducted. The SP duration of time 0 to 9 min led to a nearly 27 percent rise in surface microhardness (of approximately 92 to about 117 HV) as well as a 14.7 percent greater enhancement in tensile strength coupled with a significant improvement in fatigue life over the entire stress range examined. During the same peening time, the density of the current corrosion reduced approximately by 71% (77.17 to approximately 22.19 $\mu\mathrm{Acm}^{-1}$), and the rate of corrosion also dropped accordingly.

According to these results, there is a high negative correlation between surface hardening and corrosion kinetics. Conversely, the peening time was increased to 12 min, which resulted in a sharp rise in the roughness of the surface by almost 98 percent over the 9 min control with no significant decrease in fatigue performance, although the density of corrosion current continued to drop. This trade-off is quantitatively shown by this divergence between the residual strengthening and the roughness-induced damage at longer peening times. On the whole, there is also a definite monotonic correlation between surface hardness and corrosion current density and optimality of fatigue performance regulated by the balance of surface hardening and roughness development.

The joint analysis shows that there is a sharp performance band where positive residual strengthening prevails over the degradation caused by roughness. A mid-range peening time (9 min) offers the most desirable compromise, with the greatest tensile strength and fatigue life with a much better corrosion resistance. Oppositely, extended peening (12 min) has the same effect of increasing corrosion resistance but reducing mechanical integrity because of overly coarse surfaces. This unifying model balances the seemingly conflicting trends in mechanical, fatigue and corrosion outcomes and gives a consistent mechanistic account as to why there is an optimum processing window.

However, it is important to note that residual compressive stresses are not taken into account directly in the current research. Based on this, resilience effects will be discussed within well-established SP processes that involve, according to the existing literature, both plastic deformation of a surface layer and work hardening, always alongside formation of a region of residual compressive stresses. Based on findings of this research, an increase in surface microhardness, along with improvement of both fatigue resistance and corrosion resistance, provides an indirect proof of these effects. Thus, residual compressive stresses could be an arguable factor.

4 Conclusion

The effect of SP duration on the mechanical, electrochemical, and surface characteristics of AA6061-T6 aluminum alloy in an alkaline chloride solution (pH = 9) was investigated in this study. SP significantly improved the surface integrity of the alloy by inducing dislocations, creating compressive residual stresses, and increasing surface hardness. The optimal balance of mechanical and electrochemical performance was achieved at a peening duration of approximately 9 minutes. At this condition, the UTS increased from 272 to 312 MPa (+14.7%), surface microhardness rose from 91.98 to 116.87 HV (+27.0%), and fatigue resistance improved by 16.7% compared with the non-shot peened corroded condition. In addition, corrosion current density decreased from 77.17 to 22.19 $\mu\mathrm{A} \cdot \mathrm{cm}^{-2}$ ($\approx$71% reduction), indicating enhanced passive film stability and improved corrosion resistance.

Extending the peening duration to 12 minutes further reduced the corrosion current; however, excessive surface roughness ($\approx$98% increase relative to 9 min) led to slight degradation in tensile and fatigue performance, suggesting that over-peening can damage the surface and induce stress relaxation.

Overall, controlled SP enhances AA6061-T6's mechanical strength, surface hardness, fatigue life, and corrosion resistance, making it a reliable choice for advanced engineering applications requiring durability in alkaline chloride environments. The complementarity of experimental techniques, including surface characterization, mechanical testing, and electrochemical analysis, allowed a thorough assessment of the interplay between residual strengthening and surface roughening effects, providing a solid fundamental understanding of the peening-induced surface strengthening mechanism.

Author Contributions

Conceptualization, K.M.K. and M.A.A.; methodology, K.M.K. and M.A.A.; validation, M.A.A.; formal analysis, K.M.K.; investigation, K.M.K. and A.M.F.; resources, M.A.A.; data curation, K.M.K. and A.M.F.; writing—original draft preparation, A.M.F.; writing—review and editing, A.M.F.; visualization, K.M.K.; supervision, M.A.A.; project administration, M.A.A. All authors were actively involved in discussing the findings and refining the final manuscript.

Data Availability

The data used to support the research findings are available from the corresponding author upon request.

Conflicts of Interest

The authors declare no conflict of interest.

Acknowledgements

The authors would like to thank Mustansiriyah University (www.uomustansiriyah.edu.iq), College of Engineering, Department of Materials Engineering, Baghdad- Iraq, for its support in the present work.

References

[1] C. Agustán-Sáenz, P. Santa Coloma, F. J. Fernández-Carretero, F. Brusciotti, and M. Brizuela, "Design of corrosion protective and antistatic hybrid sol-gel coatings on 6XXX AlMgSi alloys for aerospace application," *Coatings*, vol. 10, no. 5, p. 441, 2020. https://doi.org/10.3390/coatings10050441

[2] K. Hariharan and S. Virtanen, "Microstructure engineering for corrosion resistance in structural alloy design," *npj Mater. Degrad.*, vol. 8, no. 1, p. 115, 2024. https://doi.org/10.1038/s41529-024-00533-y

[3] N. Zhou, "Microstructure-property development and defect characterization of Al-X friction welds for automotive applications," Master's thesis, University of Birmingham, 2020. http://etheses.bham.ac.uk/id/eprint/10186

[4] O. S. MacGregor, "Evaluating the wear and corrosion resistance of plasma-sprayed tungsten carbide coatings on aluminium-6082 alloy," Master's thesis, University of the Witwatersrand, Johannesburg (South Africa), 2017. https://www.proquest.com/openview/a4ccb146aa71f2c99d303193f5793c97/1?pq-origsite=gscholar&cbl=2026366&diss=y#

[5] L. Li, "Corrosion protection provided by trivalent chromium process conversion coatings on aluminum alloys," Ph.D. dissertation, Michigan State University, 2013.

[6] L. Malagutti, G. Ronconi, M. Zanelli, F. Mollica, and V. Mazzanti, "A post-processing method for improving the mechanical properties of fused-filament-fabricated 3D-printed parts," *Processes*, vol. 10, no. 11, p. 2399, 2022. https://doi.org/10.3390/pr10112399

[7] S. K. Spanrad, "Fatigue crack growth in laser shock peened aerofoils subjected to foreign object damage," Ph.D. dissertation, University of Portsmouth, 2011. https://pure.port.ac.uk/ws/portalfiles/portal/6061408/Sven.Spanrad.PhD_Thesis_2011.pdf

[8] Q. Pu, J. Qian, Y. Zhang, S. Yang, H. Huang, Q. Chao, and G. Fan, "The influence of post-treatment on micropore evolution and mechanical performance in AlSi10Mg alloy manufactured by laser powder bed fusion," *Materials*, vol. 17, no. 17, p. 4319, 2024. https://doi.org/10.3390/ma17174319

[9] Pranowo, F. Soesianto, and B. Suhendro, "Simulating seismic wave propagation in two-dimensional media using discontinuous spectral element methods," in *Proceedings of International Conference on Applied Mathematics*, Bandung, Indonesia, 2025. https://repository.uajy.ac.id/id/eprint/13772

[10] D. R. Tenney, E. A. J. Starke, J. C. N. Jr., J. Heyman, and T. T. Bales, "Structural Framework for Flight II: NASA's Role in Development of Advanced Composite Materials for Aircraft and Space Structures," NASA Technical Reports Server, 2019. https://ntrs.nasa.gov/api/citations/20190002562/downloads/20190002562.pdf

[11] E. Salvati, "Evaluating fatigue onset in metallic materials: Problem, current focus and future perspectives," *Int. J. Fatigue*, vol. 188, p. 108487, 2024. https://doi.org/10.1016/j.ijfatigue.2024.108487

[12] J. Waller and S. James, "ASTM E07 Committee on Nondestructive Testing Activities," NASA Technical Reports Server, 2015. https://ntrs.nasa.gov/api/citations/20150019622/downloads/20150019622.pdf

[13] S. Alkunte, I. Fidan, V. Naikwadi, S. Gudavasov, M. A. Ali, M. Mahmudov, and M. Cheepu, "Advancements and challenges in additively manufactured functionally graded materials: A comprehensive review," *J. Manuf. Mater. Process.*, vol. 8, no. 1, p. 23, 2024. https://doi.org/10.3390/jmmp8010023

[14] R. Sun, Z. Cao, Y. Zhang, H. Zhang, Y. Yu, Z. Che, and W. Guo, "Laser shock peening of SiCp/2009Al composites: Microstructural evolution, residual stress and fatigue behavior," *Materials*, vol. 14, no. 5, p. 1082, 2021. https://doi.org/10.3390/ma14051082

[15] C. H. Su, T. C. Chen, Y. S. Ding, G. X. Lu, and L. W. Tsay, "Effects of micro-shot peening on the fatigue strength of anodized 7075-T6 alloy," *Materials*, vol. 16, no. 3, p. 1160, 2023. https://doi.org/10.3390/ma16031160

[16] L. Sheng-Li, Y. Cui, X. Gao, and T. S. Srivatsan, "Influence of exposure to aggressive environment on fatigue behavior of a shot peened high strength aluminum alloy," *Mater. Sci. Eng. A*, vol. 574, pp. 243–252, 2013. https://doi.org/10.1016/j.msea.2013.02.055

[17] W. Huang, B. Leister, N. Shen, A. Mckee, S. Mubeen, G. Bonheyo, and H. Ding, "Enhancing corrosion resistance of lightweight metal alloys through laser shock peening," *J. Laser Appl.*, vol. 36, no. 4, p. 042040, 2024. https://doi.org/10.2351/7.0001541

[18] ASTM International, "Standard Specification for Aluminum and Aluminum—Alloy Sheet and Plate," West Conshohocken, PA, USA, 2014. https://store.astm.org/b0209-14.html

[19] ASTM International, "Standard Practice for Calculation of Corrosion Rates and Related Information from Electrochemical Measurements," West Conshohocken, PA, USA, 2023. https://store.astm.org/g0102-23.html

[20] ASTM International, "Standard Test Methods for Tension Testing Wrought and Cast Aluminum-and Magnesium-Alloy Products (Metric)," West Conshohocken, PA, USA, 2015. https://store.astm.org/b0557m-15r23.html

[21] "Standard Test Method for Microindentation Hardness of Materials."

[22] International Organization for Standardization, "Geometrical Product Specifications (GPS)—Surface Texture: Profile Method—Terms, Definitions and Surface Texture Parameters," Geneva, Switzerland, 1997. https://cdn.standards.iteh.ai/samples/62307/a134269fdf9d45d19855b7361576a651/ISO-4287-1997-DAmd-2.pdf

[23] A. Bag, D. Delbergue, J. Ajaja, P. Bocher, M. Lévesque, and M. Brochu, "Effect of different shot peening conditions on the fatigue life of 300 M steel submitted to high stress amplitudes," *Int. J. Fatigue*, vol. 130, p. 105274, 2020. https://doi.org/10.1016/j.ijfatigue.2019.105274

[24] J. A. Granato, J. A. Pontes, E. P. Gonçalves, and V. Sinka, "Excessive coverage effect (over peening) in the blasting operation of aluminum alloy 'AA 7475-T7351' with steel shot," *Matéria (Rio J.)*, vol. 25, no. 2, pp. e–12 614, 2020. https://doi.org/10.1590/S1517-707620200002.1014

Nomenclature

Latin Symbols

UTS	Ultimate tensile strength (MPa)
Nf	Number of cycles to failure
Ra	Surface roughness (arithmetic mean) (μm)
HV	Vickers microhardness (HV)
CR	Corrosion rate (mm/year)
EW	Equivalent weight (g/equiv)
ρ	Density ($\mathrm{g/cm^3}$)
OCP	Open-circuit potential (V)
SP	Shot peening
v	Shot impact velocity (m/s)
t	Shot peening time (min)
d	Shot diameter (mm)
pH	Alkalinity level of solution
SCE	Saturated calomel electrode
NaCl	Sodium chloride solution (3.5 wt%)
$\mathrm{NaHCO_3}$	Sodium bicarbonate

Greek Symbols

σ	Stress amplitude (MPa)
φ	Nozzle inclination angle (degrees)
μA	Microampere (μA)
α	Anodic slope (Tafel) (V/dec)
β	Cathodic slope (Tafel) (V/dec)

Subscripts

Ecorr	Corrosion potential (V (SCE))
icorr	Corrosion current density ($\mu\mathrm{A/cm^2}$)
ic	Corrosion current (μA)
η	Overpotential (V)
corr	Corrosion-related parameter
f	Fatigue measurement